eISSN: 2976-1190

Journal of Engineering and Sciences

Vol. 4, Issue 2, Nov 2025, 171-186

DOI: https://doi.org/10.3126/jes2.v4i2.82124

Journal homepage: Journal of Engineering and Sciences (nepjol.info)

Publisher: Research Management Cell, Paschimanchal Campus, Lamachour, Pokhara

Predicting Mass Balance of Glaciers in the Central Himalaya Region using Machine Learning

Sakchhyam Gurung[1,*], Bidur Devkota[1], Ranjan Adhikari[1], Rammani Adhikari[2]

[1]*Gandaki College of Engineering and Science, Pokhara University, Pokhara, Nepal*

[2]*School of Engineering, Pokhara University, Pokhara, Nepal*

[*]*Corresponding author: sakchhyamgurung3@gmail.com*

(Manuscript Received: 14/08/2025; Revised: 27/11/2025; Accepted: 30/11/2025)

Abstract

Glaciers serve as critical indicators of climate change worldwide, and with rapid glacier melt and increased vulnerability to Glacial Lake Outburst Floods (GLOFs), it is necessary to assess regions like High Mountain Asia (HMA), which hosts a dense concentration of glaciers and glacial lakes, for glacier health. One key metric is the Glacier Mass Balance (GMB), which represents the net mass gain or loss of a glacier over a given year. While traditional temperature-index-based machine learning models have been developed for GMB prediction, the influence of energy balance and solar radiation—especially at low latitudes—remains underexplored. This study predicts the GMB for low-latitude HMA glaciers using machine learning models, including Linear models, XGBoost, and Multi-Layer Perceptron (MLP). The dataset for the model includes key feature groups, including topographic, meteorological, and radiation. The target variable for training and evaluation was derived from the Hugonnet glacier mass balance dataset (2000–2019). To prevent data leakage and ensure spatial robustness, glacier-aware dataset splitting methods such as StratifiedGroupKFold were used. Among the models tested, XGBoost performs best with an R^2 of 0.559 and RMSE of 0.259, followed by MLP (R^2 = 0.0.512 and RMSE 0.273). Linear models (Ridge and Lasso) perform the worst, with similar R^2 values of 0.335 and RMSE of 0.319. Feature importance and SHAP value analysis reveal that latitude, longitude, and topological features are dominant predictors, highlighting the role of geographic location in glacier dynamics, mainly in low-latitude Himalayan regions. Overall, this study demonstrates the use of solar radiation and climate features for predicting GMB and investigates their role in the overall influence on GMB prediction at the low-latitude HMA glacier.

Keywords: Glacier; Energy Balance; High Mountain Asia; ERA5-Land; Glacier Mass Balance; XGBoost; Regression

1 Introduction

High Mountain Asia (HMA), encompassing parts of Nepal, India, Pakistan, Bhutan, China, and several Central Asian countries, is characterized by its vast high-elevation terrain, prominent mountain ranges, and dense glacier coverage. As one of the largest reservoirs of snow and ice outside the polar region, HMA serves as a critical freshwater source for downstream populations (*HighMountainAsia*, n.d.). Approximately 250 million people rely on HMA glacier melt for seasonal water security (*Health and Sustainability of Glaciers in High Mountain Asia | Nature Communications*, 2021). The region can be further subdivided into zones, such as the Central Himalayas, Inner Tibet, and the Hindu Kush, each with unique glaciological and hydrological characteristics.

The formation and evolution of a glacier are influenced by the balance between the mass it gains and the mass it loses due to melting. The term "*glacier mass balance*" (GMB) refers to the rate of glacier mass change per unit area, measured in meters of water equivalent (m w.e.) per year. Essentially, mass balance indicates the 'health' of a glacier: glaciers that lose more mass than they gain experience a negative mass balance and consequently recede, while those that gain more mass than they lose have a positive mass balance and thus advance (Davies, 2020). For example, the well-studied Yala Glacier in the Langtang region of Nepal has an average mass balance of -0.80 ± 0.28 m w.e. yr-1 from 2011 to 2017 and has cumulatively lost approximately -12.9 m w.e. since 2000, with summer ablation being the most dominant process (Stumm et al., 2021). Glacier mass balance is a vital indicator because it responds instantly to atmospheric forcing and links changes in the cryosphere to climate monitoring (Stumm et al., 2021).

This research used various machine learning (ML) models to examine predictors of GMB in the low-latitude HMA region and investigate the possible role of radiation features in GMB. The study's primary focus is on using topological, meteorological, and radiation features to predict GMB, an integer-valued variable, thereby treating it as a regression problem. Additionally, explainable plots, such as SHAP (Shapley Additive Explanations) and ALE (Accumulated Local Effects), were used to visualize feature contributions to model predictions.

2 Literature Survey

Conventional mass balance measurements rely on in-situ staking methods (Davies, 2020; *Glacier Mass Balance - an Overview | ScienceDirect Topics*, n.d.; Ren et al., 2024), geodetic DEM (Digital Elevation Model) differencing (Stumm et al., 2021; Zemp et al., 2009), and physical models, such as energy balance (Che et al., 2019) or temperature index models. However, these approaches are often constrained by their spatial coverage, data requirements, and computational complexity (Bolibar et al., 2020; Ren et al., 2024).

Recent advances in ML have introduced promising alternatives for estimating glacier mass balance. ML models, including gradient boosting trees (Ren et al., 2024) and deep neural networks have demonstrated superior performance in capturing the nonlinear dynamics of glacier systems (Bolibar et al., 2020), offering a scalable, data-driven approach to mass-balance prediction across heterogeneous glacial environments. But, studies on GMB prediction have predominantly focused on high-latitude regions of the HMA, often relying on traditional temperature-index models that use predictors such as cumulative positive temperature (CPT) and precipitation (Peng et al., 2025; Ren et al., 2024). While surface energy balance (SEB) components, such as shortwave and longwave radiation, are recognized as essential drivers of glacier melt (Diaconu & Gottschling, 2024). Their inclusion in predictive models remains limited due to the complexity and sensitivity of the modeling process.

Notably, studies using machine learning for GMB prediction have primarily focused on regions such as the French Alps (Anilkumar et al., 2023; Bolibar et al., 2020, 2022), and the Swiss Alps (van der Meer et al., 2025). The HMA-focused studies primarily model high-latitude glaciers and glacial lake dynamics (Hartmann, 2022; Ren et al., 2024) and often omit critical SEB parameters. Furthermore, within HMA, regions at lower latitudes, such as Nepal, remain underexplored despite their distinct topographic and climatic conditions, which may significantly influence glacier behavior. In Nepal, the use of Google Earth Engine (GEE) has been confined mainly to mapping applications, such as glacier delineation and glacial lake monitoring (J. Zhang et al., 2021; M. Zhang et al., 2022), weather monitoring (Thapa & Devkota, 2024), location mapping applications (Devkota et al., 2019), etc., rather than predictive modeling through ML approaches.

Another methodological limitation in existing ML studies is the frequent practice of pooling all glacier data together(Anilkumar et al., 2023; Ren et al., 2024), which increases the risk of data leakage and overestimation of model performance. A more robust approach would treat each glacier as an independent spatiotemporal unit of data, ensuring generalizability and avoiding inadvertent information leakage during training and testing.

Climate in the lower HMA region, such as the Himalaya region, is heavily influenced by the South Asian summer monsoon (ISM) and Westerly Disturbances (WDs). ISM is driven by the contrast in land-sea temperatures, which draws moisture southwesterly winds from the Indian Ocean, causing precipitation (Dimri et al., 2015). Typically, ISM starts in June, with early withdrawals in September. For low altitude regions, such phenomena cause heavy rainfall, but for high-altitude glaciers, precipitation falls as snow (above Equilibrium Line Altitude (ELA)) and accumulates (Dimri et al., 2015; Loo et al., 2015). During winter, WDs originating in the Mediterranean bring moisture to the western Himalaya, including the Karakoram and Hindu Kush, leading to glacier accumulation in an otherwise cold and dry season. It lasts from December to March (Dimri et al., 2015; Loo et al., 2015).

3 Materials and Methods

3.1 Study Area

The study area, as shown in Figure 1, focuses on the lower latitudes of the HMA region, including the Central Himalaya, East Himalaya, West Himalaya, Karakoram, Hengduan Shan, and Hindu Kush. This region features high peaks ranging from 7,000 to 8,000 meters in elevation, high-altitude glacial lakes, and extensive glaciers. The study area spans multiple countries, including Nepal, India, China, Bhutan, Afghanistan, and Pakistan. To ensure accurate glacier delineation and compatibility among different data sources, the Global Glacier Boundary 2023, provided by the Global Terrestrial Network for Glaciers (GTN-G), was utilized.

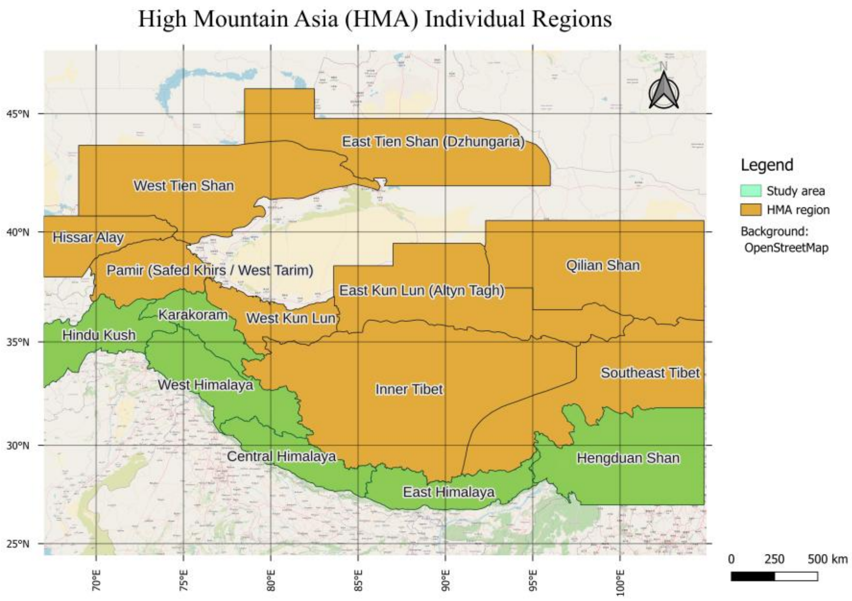

Figure 1: Study Area, HMA

3.2 Dataset Collection

The data collected for the study focuses on the lower-latitude HMA region. The dataset's period is constrained by the availability of the target variable, i.e., mass balance. Since the mass balance observation, sourced from (Hugonnet et al., 2021), spans from 2000 to 2019 and refers to glacier IDs and outlines from the Randolph Glacier Inventory (RGI) version 6.0, the meteorological and radiation data will also span the same timeline.

The variables used are mainly categorized into topological, glaciological, climatic, and radiation features. Ultimately, all the features fall under either ablation or accumulation variables. Ablation refers to the processes that melt glacier ice, whereas accumulation refers to the processes that add ice to the glacier system. An overview of the variables used in this study is shown in Table 1.

Table 1: Ablation and Accumulation Variables

Topographical Variables	**Ablation Variables**	**Accumulation Variables**
- Longitude, Latitude - Area - Altitude: Med - Slope - Cosine Aspect - Flow-line length - ELA - Mean glacier velocity - Z-range - ELA proximity	- Surface temperature: seasonal - CPT: seasonal - Surface latent heat flux (SLHF): seasonal - Surface sensible heat flux (SSHF): seasonal - Surface net solar radiation (SSR): seasonal - Surface net thermal radiation (STR): seasonal	- Snow depth: seasonal - Precipitation: seasonal, winter monsoon, and summer monsoon

3.2.1 Glacier Inventory (RGI 6.0): Outline and Topology

The RGI provides glacier outlines and topographic variables for global glaciers. We focus on regions 14 and 15, highlighted in Figure 2, which comprise over 41,000 glaciers. Figure 3 provides a closer look at an outline of one of the famous glaciers in the Everest region of Nepal, the Khumbu glacier.

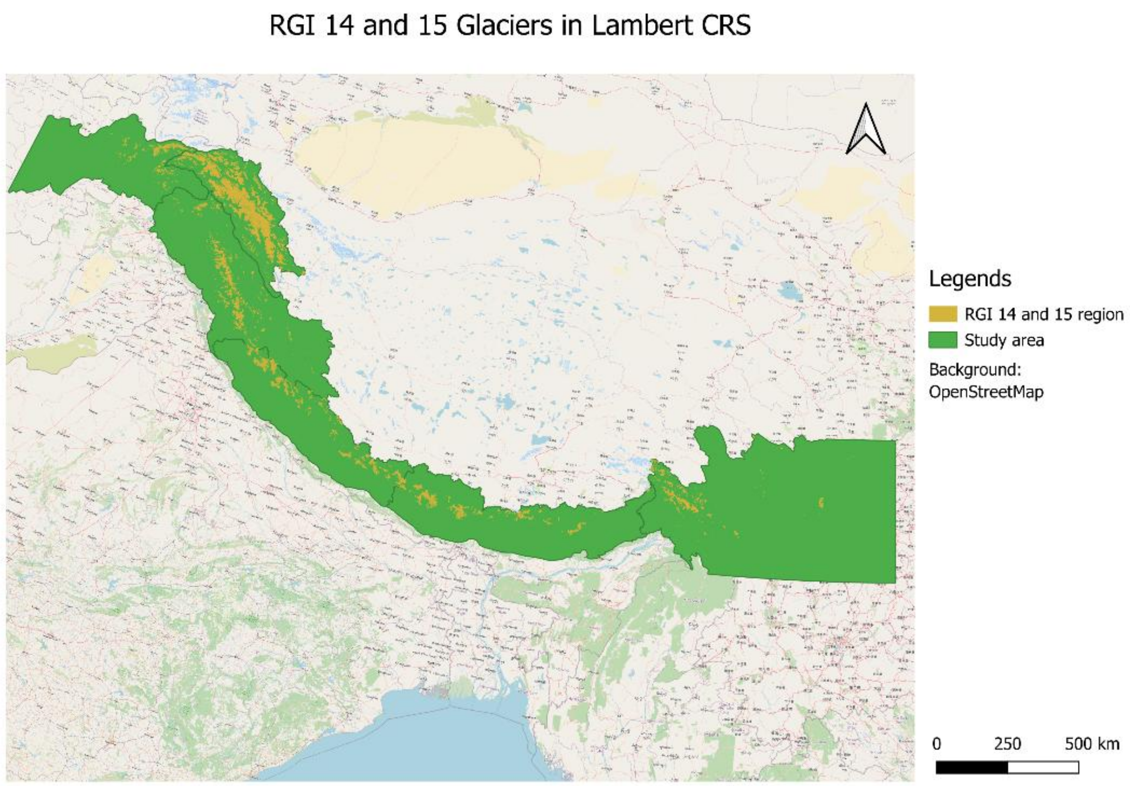

Figure 2: RGI 14 and 15 glaciers in Lambert projection

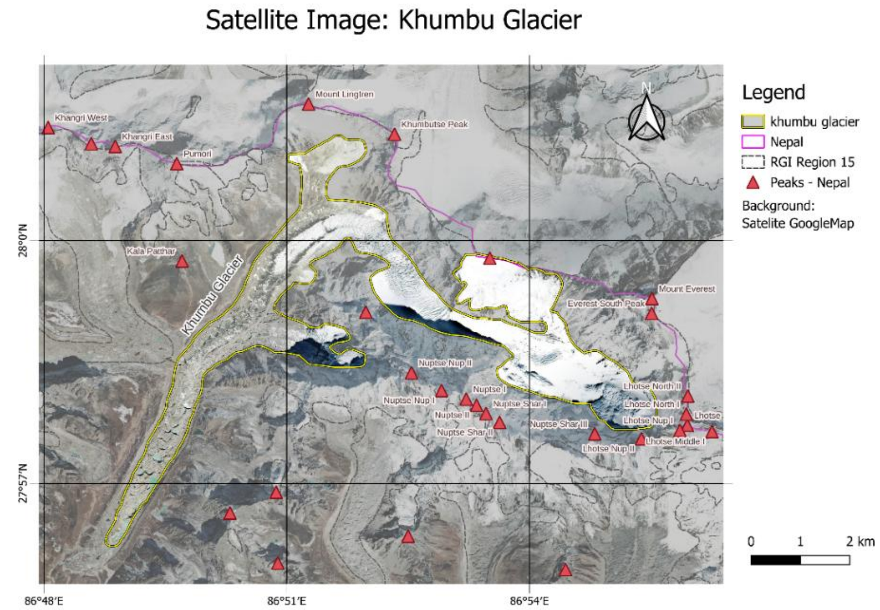

Figure 3: A close-up of Example Glacier: Khumbu Glacier Region 15

3.2.2 Mass balance observations

Mass balance ($dmdtda$) represents specific mass change ($kg\ m^{-2}\ yr^{-1}\ or\ m\ w.e. yr^{-1}$) and is used as the target variable. The study by (Hugonnet et al., 2021) provides data spanning 2000-2019, capturing long-term trends in glacier mass change.

3.2.3 ERA-Land reanalysis data

ERA5-Land (The European Centre for Medium-Range Weather Forecasts, version 5) is a reanalysis dataset that provides a consistent view of the evolution of land variables over several decades. In this study, we used monthly-averaged data because our goal is to obtain seasonal aggregations of radiation variables, snow depth, and climate-forcing indicators, such as total precipitation and surface temperature.

3.3 Methodology

As illustrated by Figure 4, the raster file undergoes geo-processing steps, including reprojection, bilinear interpolation, and zonal statistics, to obtain the per-glacier feature value. The vector files are reprojected and typically used to delineate the raster file within our area of interest or glacier. Since our study focuses on the lower-latitude region of the HMA, we used *EPSG:102012 (Asia Lambert Conformal Conic)* as the common Coordinate reference system (CRS). Additionally, due to the coarse ERA-5 resolution (approximately 9 km), bilinear interpolation was applied to resample the raster data to a 1 km × 1 km grid, thereby improving the representativeness for smaller glaciers (Ren et al., 2024). The Khumbu glacier is shown in Figure 3 has an input raster (Figure 5), which is processed to produce the raster shown in Figure 6. The processed raster is converted to a tabular format by taking the mean of all raster pixels within the glacier's outline.

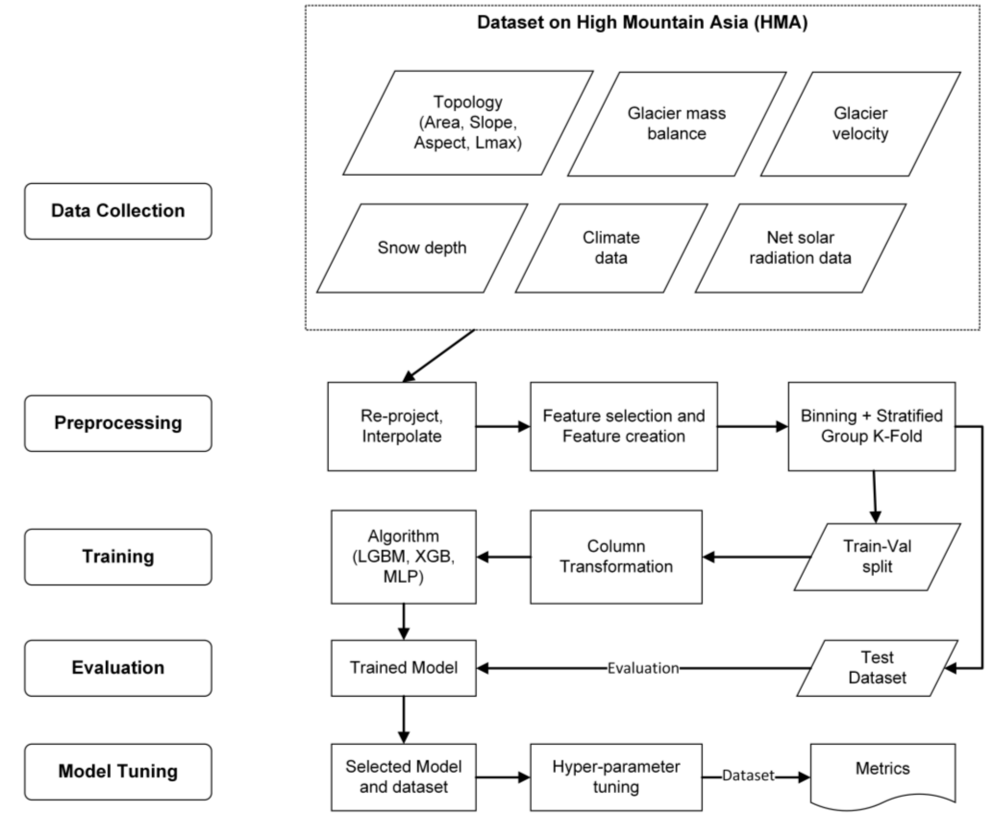

Figure 4: Methodology of the study

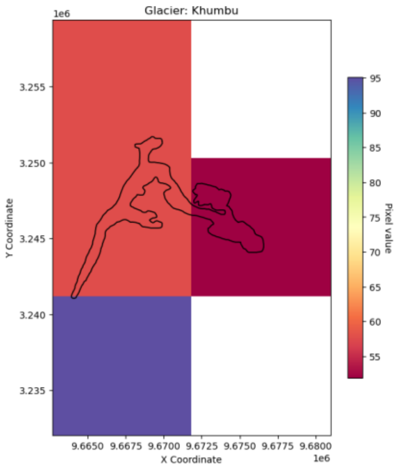

Figure 5: XY grid of Khumbu glacier before pre-processing

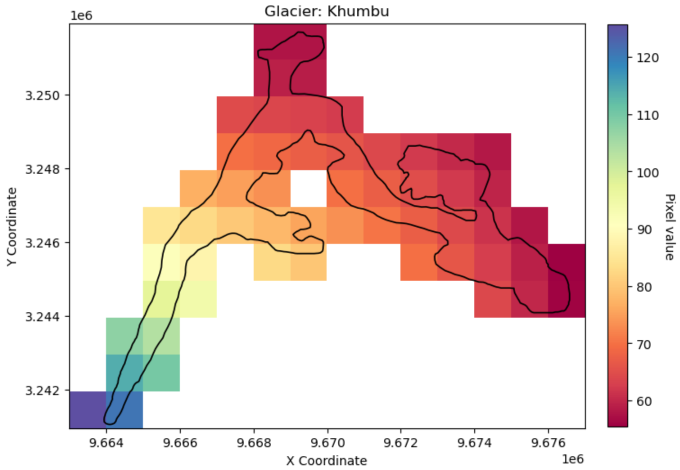

Figure 6: XY grid of Khumbu glacier after re-projection, bilinear interpolation, and raster clipping

3.3.1 Data preprocessing

All tabular datasets, including topological, ELA, glacier velocity, climate, and radiation, are merged into a single table based on glaciers' RGI IDs and years. The merged tabular data is generally checked for empty fields, invalid data types, and time-range compatibility. The data undergoes unit conversion (e.g., Kelvin to Celsius), filtration, and other processing steps to meet our criteria. To adjust for the coarseness of the resampled raster grid, glaciers greater than or equal to 1 square km were selected; an overview of total glaciers at this stage is provided in

Table 2. The ready dataset can now be explored and analyzed, or further processes, such as feature creation and elimination, can be performed.

Table 2: An overview of the Dataset Before and After Area Constraint

Region	Total Glaciers	After Data Cleaning	Area >= 1 sq. km	Predictors
14	27,988	8,056	4,570	-
15	13,119	4,432	2,576	-
Total	**41,407**	**12,488**	**7,146**	**41**

3.3.2 Feature Engineering

New features were added to enhance the model's predictive power and capture a more accurate relationship between the derived features and the target variable. Table 3 provides an overview of the derived features.

To address noise and biases in the dataset derived from climate variables, anomalies were calculated for each climate and radiation feature by subtracting each variable's average over a chosen reference period (20 years in this case), as shown in equation (1) (Bolibar et al., 2020). The *delta* prefix in the dataset indicates the presence of anomalies.

Delta of a variable = value of variable – average of variable over 20 yrs (1)

Table 3: An overview of Derived features

Feature Group	Feature	Description
Cosine Aspect	cosine_aspect	Cyclic pattern scaled to cosine values between -1 and +1.
Altitude related	z_range, ela_proximity	Quantify relative glacier elevation with respect to the ELA.
Mu	mu_<feature_name>	20-year average of climate and radiation features
Delta	delta_<feature_name>	Deviation of yearly climate or radiation features from the 20-year average

3.3.3 Algorithm selection

To model GMB across the low-latitude HMA region, three machine learning algorithms were selected: Two linear models, Ridge and Lasso regression models, Extreme Gradient Boosting (XGBoost) (Chen & Guestrin, 2016), and a Multi-Layer Perceptron (MLP) neural network (Bishop & Bishop, 2024). The linear models were selected to capture the linear relationships in the dataset. The XGBoost model was chosen for their ability to handle high-dimensional tabular data and robustness to noise. At the same time, the MLP model was selected for its ability to capture complex nonlinear relationships between predictors and target variables.

Ridge and Lasso regression models, also known as L2 and L1 regularization, respectively, introduce penalty terms into the model's loss function to avoid overfitting and improve predictive performance.

XGBoost is an ensemble tree-based model that utilizes the gradient boosting method to improve performance by using a sequential ensemble of multiple weak learners. Tree-based models don't need feature scaling and are robust to noise.

The MLP model was employed to explore the performance of deep learning methods in glacier mass balance prediction, leveraging its ability to capture non-linear relationships that decision trees may not easily model. Unlike linear models and tree-based models, MLP doesn't need linear combinations of predictors. Generally, the hidden layers and neurons within each layer select the combination of feature variables (Bolibar et al., 2020).

3.3.4 Splitting approach

When reviewing many studies, very few consider each glacier as a single source of data. Instead, the train, validation, and test splits are randomly shuffled, thereby creating data leakage (Anilkumar et al., 2023). Therefore, the model performs well but is not robust to unseen glaciers.

Considering the spatial nature of glaciers, we have treated each glacier as an independent data source. It means a glacier in the training set cannot appear in the testing set during model development. Such a strict separation of glaciers will ensure the generalizability of the model and prevent inadvertent information leakage during training and testing (Bolibar et al., 2020).

Stratified K-Fold splitting based on glacier-wise median mass balance binning, i.e., calculating a median of a glacier's entire timeline and splitting on that basis. The dataset was divided into train, validation, and test sets in the ratio of 50:20:30. This prevents data leakages and ensures a balanced spread of representative mass balance samples in each of the train-validation-test splits.

The model's performance is evaluated based on commonly used regression metrics, such as R^2, which determines the variance explained by the model, and $RMSE$, which defines the model's fitness.

3.3.5 Hyperparameter Tuning

In this study, based on the baseline performance of each model in each dataset variation, the best model and dataset variation were selected. Then, for initial tuning, the Ray tune library, combined with the ASHA (Async Hyper Band Scheduler) scheduler (Li et al., 2020) and the Hyperopt search algorithm (Bergstra et al., n.d.), was used for selected models and dataset variation models.

For the ridge and lasso regularized models, the lambda (λ) parameter with sklearn's GridSearchCV was used due to the low cost of computation in these models. Tree models primarily rely on hyperparameters, such as boosting iterations, learning rate, and maximum depth (i.e., the depth of the tree and the number of leaves), as well as regularizations. So, a search space for different hyperparameters was defined. MLP model hyperparameter tuning is more challenging than the tree-based models. The MLP model requires a balance between structural complexity (i.e., the number of hidden layers) and the selection of hyperparameters. MLP hidden layers define the depth of the model, and neurons for each hidden layer define the width of the model. The MLP structure, along with regularization parameters, learning rate, dropout rate, and activation functions, adds complexity to MLP hyperparameter tuning.

3.3.6 Performance Metrics

Given the use of metrics by other researchers and for comparative study, the following metrics are employed to evaluate the model's performance: the coefficients of determination (R^2) and Root Mean Squared Error ($RMSE$) are used as primary metrics.

R^2 measures the goodness of fit of a regression model. It ranges from 0 to 1, where one indicates that the model perfectly fits the data, and zero indicates that the model does not explain any of the variability in the data. Equation (2) explains the R^2.

$$R^2 = 1 - \frac{MSE(model)}{MSE(baseline)} = 1 - \frac{\sum_{i=1}^{n}(y_{actual} - y_{pred})^2}{\sum_{i=1}^{n}(y_{actual} - y_{actual\ avg})^2} \quad \ldots(1)$$

$RMSE$ measures the average difference between the predicted values of a model and the actual values. A lower $RMSE$ indicates better model performance. Equation (3) explains the RMSE.

$$RMSE = \sqrt{\frac{\sum_{i=1}^{n}(y_{pred} - y_{actual})^2}{n}} \quad \text{...(2)}$$

3.3.7 Analysis Methods

Analysis and interpretation methods are used to complement the evaluation metrics for the model's performance. They help to highlight and interpret the marginal effect of features on the predictive power of the model.

The gain plot shows how much a feature improves accuracy or decreases loss during tree splitting. It ranks the most important features for the model based on the given feature dataset. SHAP is an explanation method based on cooperative game theory. The SHAP approach uses input features and a trained model to fairly distribute credit for the model's output among its features. The ALE plot is a global interpretation tool. It shows trends derived from the dataset and works well even with highly correlated features. The ALE measures the local effects of a feature over small intervals and sums them up across the dataset, providing an average impact of the feature on the model's prediction.

3.3.8 Experiment Design

The study was conducted using a primary dataset covering areas greater than or equal to 1 sq. km. Different dataset variations were created based on feature set combinations, such as the *meta + topo* dataset, which includes meta data and topological features only, as presented in Table 4. This approach provided insights into the influence and dominance of different predictor groups in both interactive and isolated conditions. Each dataset variation undergoes hyperparameter tuning. The final results are discussed in the Results section.

Table 4: Dataset variations used in the study

Dataset Variation	**The feature set included**
meta_topo no loc	Meta + Topo (topology)
delta loc	Meta + Topo + Climate + Rad (radiation) + Loc (location)

4 Results and Discussion

4.1 Exploratory Data Analysis (EDA)

For EDA of the dataset and features, various plots and statistics per feature can be used to reflect the nature of the feature. We used univariate and bivariate plots for visual analysis of different features.

Most of the univariate plots of features exhibited heavy skewness and outliers, as shown in Figure 7. Such features typically introduce noise, leading to issues of overfitting or underfitting. Very few features, such as altitude and temperature, exhibit normal distribution. The primary cause of such disturbances can be attributed to the presence of extremely small or large glaciers, the challenging topography in the HMA region, and a lack of periodic in situ observations.

In a bivariate plot of features against the target variable (mass balance), few to no features exhibit a clear linear or non-linear relationship with the target variable (Figure 8), making it very difficult for the model to predict the target value with confidence.

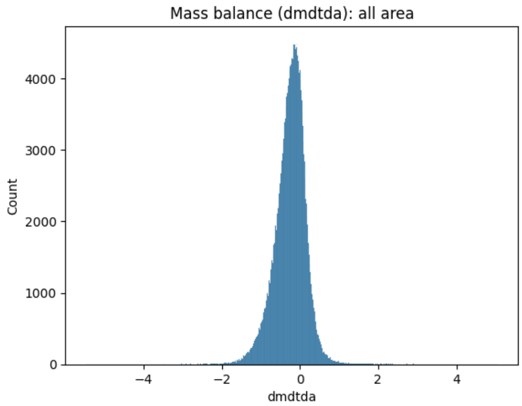

Figure 7: Univariate plots of target variable: Glacier Mass Balance (dmdtda)

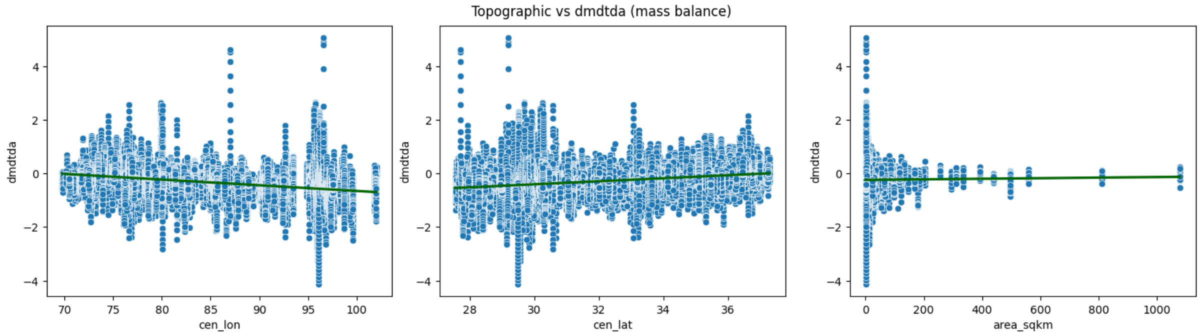

Figure 8: Bivariate plots of some topographic features against mass balance (dmdtda)

4.2 Baseline performance

To highlight the significance of dynamic drivers in modeling natural phenomena like glacier ecosystems, XGB and MLP were evaluated using only the basic features, such as meta and topological features, without any location features (*meta_topo no loc*). All evaluations were performed on glaciers with areas of 1 sq. km or more.

In this baseline,

Table 5 shows that XGB achieved an R^2 of 0.273 and an RMSE of 0.333. At the same time, MLP yielded an R^2 of 0.262 and an RMSE of 0.336. From these results, it can be concluded that the predictive power of basic features is insufficient to capture the mass balance pattern, underscoring the need for additional dynamic features, such as location, climate, and radiation.

4.3 Performance with full feature set

Table 5 displays the results of all four models on the complete feature dataset. XGB outperforms all other models with an R^2 of 0.559, with a margin of +0.047 from the second-best model, MLP, with an R^2 of 0.512. The Lasso and Ridge linear models have similar scores, with an R2 of 0.335 and an RMSE of 0.319. A comprehensive scatter plot of different models in the full feature dataset is illustrated in Figure 9.

Incorporating the full feature set yields the highest score and the greatest predictive power, particularly with tree-based XGB. XGB performance can be attributed to its robustness to noisy datasets. MLP performance was limited by sensitivity to data variability and difficulties in hyperparameter tuning. Linear models are too simple to accurately capture the relationships in the dataset.

Table 5: Model's Performance with different dataset variants

Model/Area Limit	**Dataset**	**Features**	R^2	**RMSE**
XGB	***meta_topo no loc (baseline)***	Meta + Topo	0.273	0.333
	delta loc (full feat.)	Meta + Topo + Loc + Climate + Radiation	**0.559**	**0.259**
MLP	***meta_topo no loc (baseline)***	Meta + Topo	0.262	0.336
	delta loc (full feat.)	Meta + Topo + Loc + Climate + Radiation	**0.512**	**0.273**
Ridge (L2)	***delta loc (full feat.)***	Meta + Topo + Loc + Climate + Radiation	0.335	0.319
Lasso (L1)	***delta loc (full feat.)***	Meta + Topo + Loc + Climate + Radiation	0.333	0.319

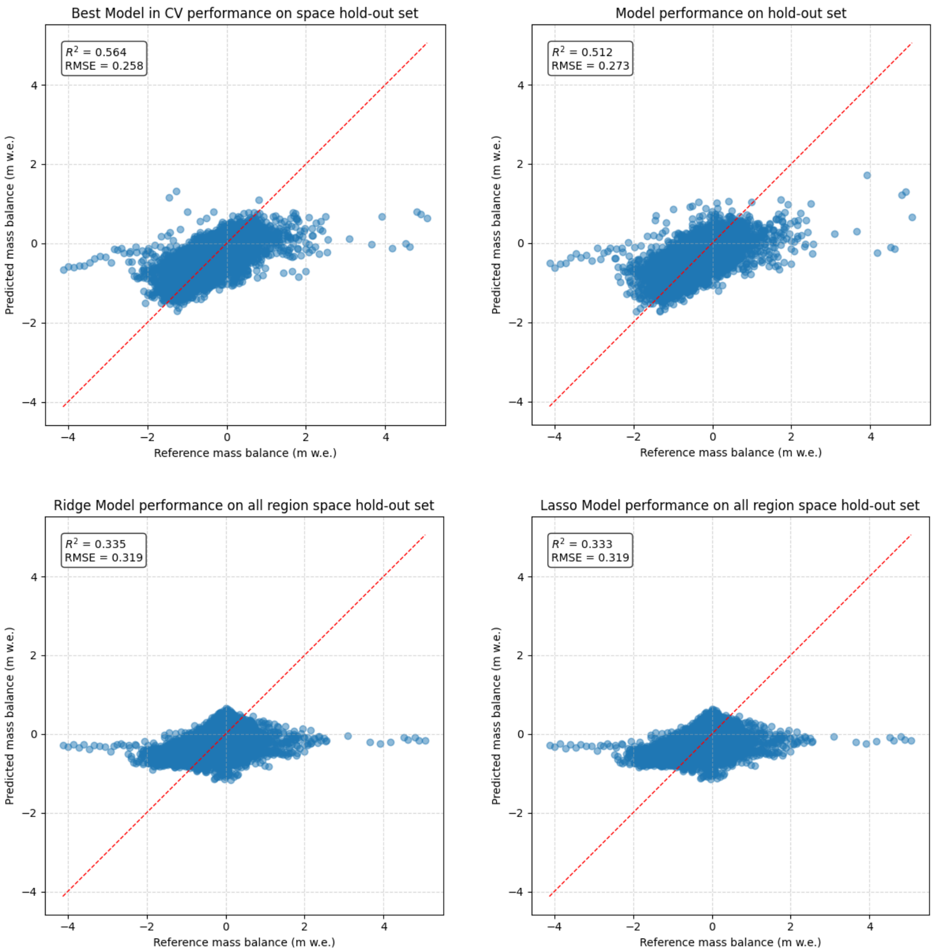

Figure 9: Predicted vs Actual mass balance for XGB, MLP, Ridge (L2), and Lasso (L1) on the full feature dataset (Area greater than or equal to 1 sq. km)

4.4 Feature Importance

The Figure 10 plot of feature importance by information gain shows central latitude as a top contributor to XGBoost predictive power, highlighting the influence of a north-south latitude gradient on climate and radiation factors. Central longitude, ranked second, also highlights the significance of an east-west gradient and its impact on climate forcing.

Other significant features include slope, ELA proximity, and median altitude, indicating the importance of topological structure in a glacier system's mass balance. Features with moderate importance include seasonal delta CPT, glacier area, and mean glacier velocity. In contrast, the less important features primarily include climate, latent heat, solar radiation, and thermal radiation.

These results indicate that, within complex glacier systems, climate and radiation forcing interact with topographic features.

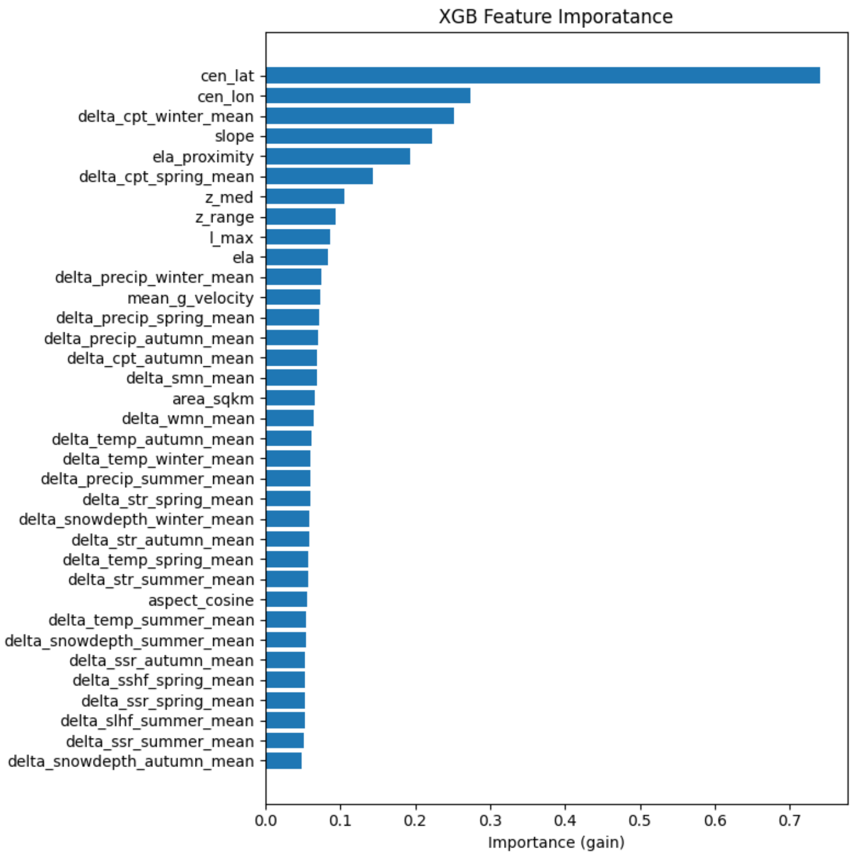

Figure 10: XGB Feature Importance (by gain) on the full feature dataset (area >= 1 sq. km)

4.5 Feature Trend

The SHAP plot in Figure 11 shows that *cen_lat, ela_proximity, slope, and cen_lon* exhibit the most variance and the most significant average SHAP values, indicating a major role in the model's decision-making. For *cen_lat*, the negative SHAP value of −0.3 (in blue) shows that a decrease in latitude value causes the model prediction value to shift down by −0.3, i.e., negative mass balance, thus implying that lower latitude glaciers have more ice melt than ice gain. In contrast, the positive SHAP value of +0.3 (in red) for the latitude feature indicates that glaciers at higher latitudes have a positive mass balance. In comparison, *cen_lon* shows the opposite influence. The further east the glacier is located, the greater the negative impact on GMB; moving west preserves ice from melting, resulting in a positive GMB. Additionally, ALE plots shown in Figure 12 for the cen_lon and cen_lat also confirm the trend. It can be concluded that the spatial distribution plays a significant role in GMB located in low-latitude regions.

However, for the radiation features, both plots, Figure 10 and Figure 11, clearly show that they lie at the lower end of the spectrum, with feature gains below 0.5. One interesting connection can be made between solar radiation's weak influence and climate aspects in low-latitude HMA. The intensity of solar radiation is directly influenced by cloud cover. During the peak monsoon season in low-latitude regions, solar radiation has less opportunity to penetrate the atmosphere. Under such conditions, due to the moist, hot air, other radiation processes, such as thermal radiation and latent heat, can take over the melting of ice or the accumulation of snow. These findings support the greater influence of climatic factors on maritime glaciers, as suggested by (Ren et al., 2024), as well as the influence of climatic events such as the seasonal monsoon (Loo et al., 2015) and WDs (Dimri et al., 2015).

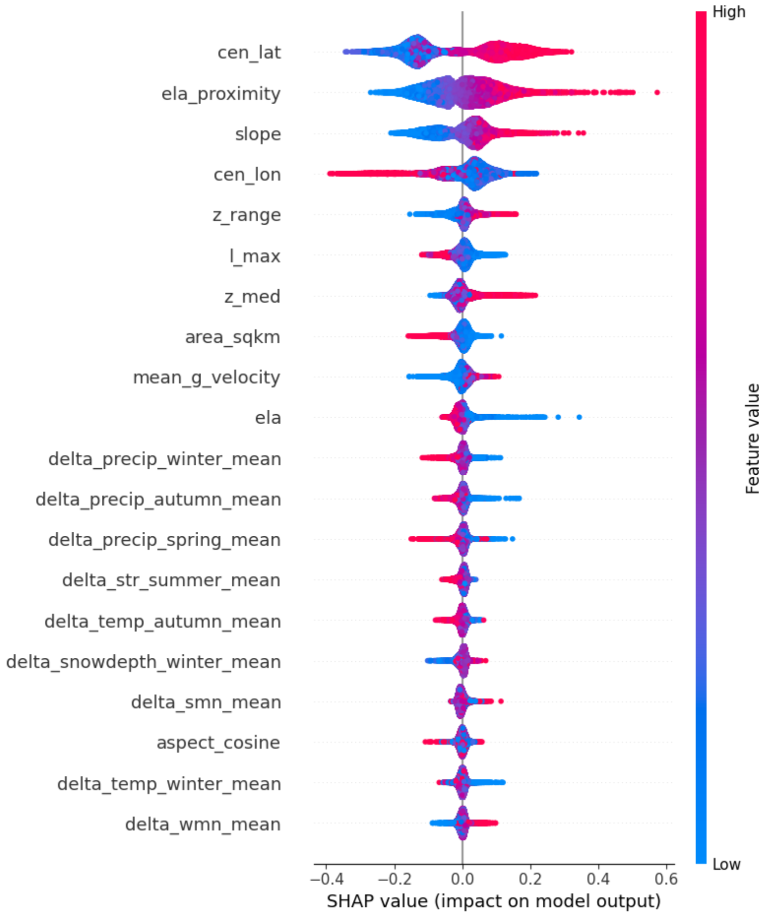

Figure 11: XGB SHAP value beeswarm plot for full feature dataset (area >= 1 sq. km)

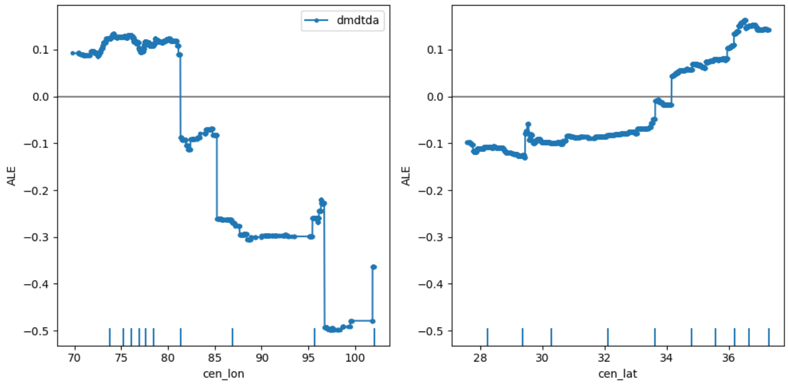

Figure 12: ALE plot for cen_lon and cen_lat using full feature dataset (area >= 1 sq. km)

4.6 Comparison with Other Studies

Studies related to GMB generally involve regional topography, climate, and datasets. Since regional variables influence glacier ecosystems, studies have customized, processed, and filtered the same reference dataset and satellite imagery in different ways. This makes it challenging to compare GMB model results across different glacier systems. (Bolibar et al., 2020) studied a very selective glacier system in the French Alps, where the MLP model scores the R^2 of 0.79 and RMSE of 0.62. Similarly, (Ren et al., 2024) focus on the maritime and continental glaciers in the higher latitude HMA region, where a tree-based Gradient Boosting Decision Tree (GBDT) model scores the $R2$ of 0.72 for the continental glacier Manas River Basin (MRB) and the $R2$ of 0.67 for the maritime glacier Niyang River Basin (NRB). The study by [11], which includes all HMA regions with an area threshold of area greater than two sq. km, reports an R2 of 0.68 with XGBoost.

Considering all this literature and the XGBoost from this study, with an R^2 of 0.559 and an RMSE of 0.259. It can be concluded that the top-performing model, the rank of feature importance, and the model's accuracy are highly dependent on the glacier system, glacier type, dataset customization, and the uncertainty associated with glaciers.

5 Limitations and Future Work

A limitation of this study is the time span of the target variable, i.e., the mass balance sourced from Hugonnet et al. (2021), which ultimately limits the time span of the predictors. Additionally, the area under study was large, and regional heterogeneity affected the model's performance, introducing conflicts in trend, pattern, and the interpretability of the final result. Moreover, at last, the native resolution of 9 km x 9 km for ERA5 Land reanalysis data is too coarse to represent the thousands of smaller glaciers.

Considering the limitations of this study and the possibilities revealed by the results, the study can focus on sub-regional areas, with a particular emphasis on high-steak glaciers and glacial lakes. Higher-resolution climate and radiation data with finer time intervals (such as weekly or monthly) can be considered, and other machine learning models can be employed.

6 Conclusion

This study found that the location and topological features of the glaciers in the low-latitude HMA region play an important role in predicting the GMB. The small glacier area and dynamic environmental conditions introduce significant uncertainty into the ML model's predictive capability. Nevertheless, the study leveraged all available resources to predict the GMB of glaciers in HMA regions 14 and 15 (area >= 1 sq. km), with a tree-based XGBoost model achieving an $R2$ of 0.559 and an RMSE of 0.259. MLP ranks second-best, with an $R2$ score of 0.512 and an RMSE of 0.273.

We can conclude that machine learning models can be used to cost-effectively predict glacier mass balance, incorporating all types of climate, radiation, and topographic features. However, a basic investment in well-balanced, high-quality, and timely remote sensing and ground data is essential for a robust and highly accurate machine learning model.

7 References

[1] National Snow and Ice Data Center. (n.d.). *High Mountain Asia*. Retrieved June 14, 2024, from https://nsidc.org/data/highmountainasia

[2] Nature Communications. (n.d.). *Health and sustainability of glaciers in High Mountain Asia*. Retrieved June 4, 2024, from https://www.nature.com/articles/s41467-021-23073-4

[3] Davies, B. (n.d.). *An introduction to glacier mass balance*. AntarcticGlaciers.org. Retrieved June 14, 2024, from https://www.antarcticglaciers.org/glacier-processes/mass-balance/introduction-glacier-mass-balance/

[4] Stumm, D., Joshi, S. P., Gurung, T. R., & Silwal, G. (2021). Mass balances of Yala and Rikha Samba glaciers, Nepal, from 2000 to 2017. *Earth System Science Data, 13*(8), 3791–3818. https://doi.org/10.5194/essd-13-3791-2021

[5] Ren, W., et al. (2024). Comparison of machine learning models in simulating glacier mass balance: Insights from maritime and continental glaciers in High Mountain Asia. *Remote Sensing, 16*(6), Article 956. https://doi.org/10.3390/rs16060956

[6] ScienceDirect Topics. (n.d.). *Glacier mass balance*. Retrieved June 15, 2024, from https://www.sciencedirect.com/topics/earth-and-planetary-sciences/glacier-mass-balance

[7] Zemp, M., Hoelzle, M., & Haeberli, W. (2009). Six decades of glacier mass-balance observations: A review of the worldwide monitoring network. *Annals of Glaciology, 50*(50), 101–111. https://doi.org/10.3189/172756409787769591

[8] Che, Y., et al. (2019). Energy balance model of mass balance and its sensitivity to meteorological variability on Urumqi River Glacier No. 1 in the Chinese Tien Shan. *Scientific Reports, 9*(1), 13958. https://doi.org/10.1038/s41598-019-50398-4

[9] Bolibar, J., Rabatel, A., Gouttevin, I., Galiez, C., Condom, T., & Sauquet, E. (2020). Deep learning applied to glacier evolution modelling. *The Cryosphere, 14*(2), 565–584. https://doi.org/10.5194/tc-14-565-2020

[10] Peng, Y., Bolch, T., Yuan, Q., Baldacchino, F., & Yang, Q. (2025). Spatiotemporal reconstruction of annual glacier mass balance in Central Asia (2000–2020) using machine learning. *Journal of Geophysical Research: Atmospheres, 130*(18), e2024JD043191. https://doi.org/10.1029/2024JD043191

[11] Diaconu, C.-A., & Gottschling, N. M. (2024). Uncertainty-aware learning with label noise for glacier mass balance modeling. *IEEE Geoscience and Remote Sensing Letters, 21*, 1–5. https://doi.org/10.1109/LGRS.2024.3356160

[12] van der Meer, M., Zekollari, H., Huss, M., Bolibar, J., Sjursen, K. H., & Farinotti, D. (2025). A minimal machine-learning glacier mass balance model. *The Cryosphere, 19*(2), 805–826. https://doi.org/10.5194/tc-19-805-2025

[13] Hartmann, D. (2022). *Impacts on glacier mass balance in High Mountain Asia assessed using machine learning* (Master's thesis). Retrieved from

https://studenttheses.uu.nl/bitstream/handle/20.500.12932/42505/ADS_Thesis_David_Hartmann_2022_.pdf

[14] Zhang, J., Jia, L., Menenti, M., Zhou, J., & Ren, S. (2021). Glacier area and snow cover changes in the range system surrounding Tarim from 2000 to 2020 using Google Earth Engine. *Remote Sensing, 13*(24), Article 5117. https://doi.org/10.3390/rs13245117

[15] Zhang, M., Chen, F., Guo, H., Yi, L., Zeng, J., & Li, B. (2022). Glacial lake area changes in High Mountain Asia during 1990–2020 using satellite remote sensing. *Research, 2022*, Article 9821275. https://doi.org/10.34133/2022/9821275

[16] Thapa, I., & Devkota, B. (2024). Applying machine learning algorithms to estimate PM2.5 using satellite data and meteorological data. *Journal of Engineering and Sciences, 3*(1), Article 66239. https://doi.org/10.3126/jes2.v3i1.66239

[17] Devkota, B., Miyazaki, H., Witayangkurn, A., & Kim, S. M. (2019). Using volunteered geographic information and nighttime light remote sensing data to identify tourism areas of interest. *Sustainability, 11*(17), 4718. https://doi.org/10.3390/su11174718

[18] Anilkumar, R., Bharti, R., Chutia, D., & Aggarwal, S. P. (2023). Modelling point mass balance for the glaciers of the Central European Alps using machine learning techniques. *The Cryosphere, 17*(7), 2811–2828. https://doi.org/10.5194/tc-17-2811-2023

[19] Dimri, A. P., et al. (2015). Western disturbances: A review. *Reviews of Geophysics, 53*(2), 225–246. https://doi.org/10.1002/2014RG000460

[20] Loo, Y. Y., Billa, L., & Singh, A. (2015). Effect of climate change on seasonal monsoon in Asia and its impact on the variability of monsoon rainfall in Southeast Asia. *Geoscience Frontiers, 6*(6), 817–823. https://doi.org/10.1016/j.gsf.2014.02.009

[21] Hugonnet, R., et al. (2021). Accelerated global glacier mass loss in the early twenty-first century. *Nature, 592*(7856), 726–731. https://doi.org/10.1038/s41586-021-03436-z

[22] Chen, T., & Guestrin, C. (2016). XGBoost: A scalable tree boosting system. In *Proceedings of the 22nd ACM SIGKDD International Conference on Knowledge Discovery and Data Mining* (pp. 785–794). https://doi.org/10.1145/2939672.2939785

[23] Bishop, C. M., & Bishop, H. (2024). *Deep learning: Foundations and concepts*. Springer. https://doi.org/10.1007/978-3-031-45468-4

[24] Li, L., et al. (2020). A system for massively parallel hyperparameter tuning. *arXiv Preprint*. https://doi.org/10.48550/arXiv.1810.05934

[25] Bergstra, J., Yamins, D., & Cox, D. D. (n.d.). Making a science of model search: Hyperparameter optimization in hundreds of dimensions for vision architectures. *arXiv Preprint*. (Original year not provided)